Received: 28 June 2023 | Revised: 18 September 2023 | Accepted: 22 September 2023

DOI: 10.1002/sfp2.1018

ORIGINAL ARTICLE

Tribology and rheology of potato protein and pectin mixtures and Maillard conjugates

Siavash Soltanahmadi[1] | **Mingxin Wang**[1] | **Mohd Khalid Gul**[1,2] | **Ecaterina Stribiţcaia**[1] | **Anwesha Sarkar**[1]

[1]Food Colloids and Bioprocessing Group, School of Food Science and Nutrition, University of Leeds, Leeds, UK

[2]Department of Food Process Engineering, National Institute of Technology, Rourkela, India

Correspondence
Anwesha Sarkar and Siavash Soltanahmadi, Food Colloids and Processing Group, School of Food Science and Nutrition, University of Leeds, Leeds LS2 9JT, UK.
Email: a.sarkar@leeds.ac.uk; s.soltanahmadi@leeds.ac.uk

Funding information
H2020 European Research Council, Grant/Award Number: 757993; UK Research and Innovation, Grant/Award Number: EP/X03514X/1; Science and Engineering Research Board

Abstract

This study aimed to compare the tribological and rheological properties of plant proteins versus their mixtures or conjugates with polysaccharides. We hypothesize that combining potato proteins (Po) with pectin (Pe) at various concentrations (0.5–5.0 wt%, ratios 1:1 and 1:2 w/w) will improve the lubrication performance of plant proteins by virtue of viscosity modification and boundary lubrication. Po showed shear thinning behavior with limited concentration-dependence in boundary and mixed lubricity. Pe on the other hand showed pronounced concentration-dependent flow and lubrication behavior delivering favorable boundary and viscous lubricity. Pe dominated the lubrication and high shear rate flow behavior in Po + Pe mixtures, governed mainly by the concentration of Pe and the hydrodynamic volume rather than the total concentration of the biopolymers. Maillard reaction (≤33% degree of conjugation) led to more negatively-charged protein-polysaccharide conjugates versus the sole biopolymers ($p < 0.05$). The conjugation decreased the second plateau shear viscosity of the Po + Pe mixtures and led to improvement in boundary and mixed lubricity when a reduced entrainment speed parameter was used. Findings from this study may inspire future studies combining plant proteins with polysaccharides to enhance their lubrication behavior and eventually improve the textural properties of plant-based foods.

KEYWORDS
friction, Maillard reaction, oral tribology, polysaccharide, plant protein, viscosity

INTRODUCTION

Tribology has been proven to be a feasible technique to give mechanistic understanding behind mouthfeel perception in orally-relevant applications spanning food (Sarkar et al., 2021; Soltanahmadi et al., 2022; Stokes et al., 2013), pharmaceutical (Batchelor et al., 2015; Hu et al., 2020) and personal care products (Zundel et al., 2018). So far, tribology, in combination with rheological assessments, has extensively contributed to understating of the correlations between the textural perception of foods and their lubrication behavior (Pradal & Stokes, 2016; Sarkar et al., 2021; Shewan et al., 2020). Particularly in food applications, tribology can be a powerful tool to help facilitating the journey toward sustainable food (Kew et al., 2021; Sarkar et al., 2021) and healthy and pleasurable food production across the lifespan (Araiza-Calahorra et al., 2023; Pradal & Stokes, 2016; Soltanahmadi et al., 2023) and understanding food adulteration and interactions between food and saliva (Biegler et al., 2016; Brown et al., 2021; Laguna & Sarkar, 2017; Shewan et al., 2020; Xu et al., 2020).

As a result of the high consumption of animal products, which are associated with high greenhouse gas emissions, a shift from an animal protein-based diet to

---

Siavash Soltanahmadi and Mingxin Wang contributed equally to this study.

a plant protein-based diet has become inevitable to produce sustainable food resources. Such a diet can have additional health benefits, such as lowering the risk of cardiovascular disease, diabetes, and other malignancies (Itkonen et al., 2021). Plant proteins are currently projected as one of alternative dietary protein sources to conventional animal proteins due to lower environmental footprints. However, often their undesirable flavor, mouthfeel perception and high oral friction have been proposed as reasons for their limited consumer acceptance (Kew et al., 2021; Saint-Eve et al., 2019; Vlădescu et al., 2023; Zembyla et al., 2021).

Potato protein (Po), extracted from by-products of the potato processing industry, is a promising protein source for human consumption due to its balanced amino acid composition, high digestibility and non-allergic characteristics (Fu et al., 2020; Hussain et al., 2021). Unlike many other plant proteins, Po has also been reported to possess excellent water solubility, gel-forming, foaming, emulsifying, antioxidant, and anticancer properties (Fu et al., 2020; Hussain et al., 2021). Recent findings have shown better lubrication and surface adsorption behavior of Po solutions as compared to other alternative proteins such as pea, insect proteins but higher friction than animal proteins (Kew et al., 2021). Hence, it was pertinent to understand whether the lubricity of the plant proteins can be improved by using combination of highly hydrated polysaccharides.

Polysaccharides are a group of food ingredients and are mainly used as thickeners, emulsifiers, gellant, encapsulants, and stabilizers (Seggiani et al., 2009) imparting desirable textural properties to food products including lubricity largely associated with viscosity component (Torres et al., 2019; You et al., 2021; You & Sarkar, 2021). Pectin (Pe) is a widely accessible and sustainable polysaccharide that is mainly composed of D-galactouronic acid residues linked together by α-(1–4) glycosidic linkages and is mainly found in the cell walls of fruits and vegetables. Pe is primarily extracted as a byproduct from citrus wastes, pulp and peel, apple pomace, and sugar-beet pulp. The water-retention and hydrogel-forming capacity of pectin (Douglas et al., 2018) makes it ideal for food products in hydrated and viscous forms and hence provides favorable viscous and lubrication properties. Pe is thus considered to be one of the most effective polysaccharides in terms of offering lubrication across the lubrication regimes and adsorption onto hydrophobic surfaces (Stokes et al., 2011).

In a complex food system, proteins can interact with several other food components such as polysaccharides, other proteins, vitamins, and minerals impacting the techno-functional, sensorial, and lubrication properties of the food system (Alves & Tavares, 2019). Such interactions depend on external factors (e.g., pH, temperature, and ionic strength) which can bring about precipitation of proteins and eventual aggregation, denaturation and coagulation (Naik et al., 2022). Proteins and polysaccharides often show synergistic effects in structuring different food systems and their electrostatic or covalent interactions (e.g., complexation) have been reported to contribute to the stability (Goh et al., 2020; Wijaya et al., 2017), and improved structural, textural and functional properties of the food (Qi et al., 2017; Setiowati et al., 2016; Souza & Garcia-Rojas, 2017) affecting the mouthfeel (Gentile, 2020; Mao et al., 2023).

In simple physical protein-polysaccharide mixtures or mixture of structured protein-polysaccharide systems (Hu et al., 2020), the interactions are mainly driven by non-covalent bonds, which are affected by pH conditions, the type of proteins/polysaccharides, their combination ratio and concentration in the mixture (Goh et al., 2020; Wijaya et al., 2017). On the other hand, heating protein-polysaccharide mixtures at an optimum pH, water activity, and time can propel covalent conjugation, referred to as Maillard-reaction. The Maillard-reaction is a food glycosylation process that results from condensation of the reducing end of a polysaccharide and deprotonation of primary amino groups of a protein (Martins et al., 2000). Such covalent conjugations are known to form stable protein-polysaccharide complexes or so-called "conjugates" (Wijaya et al., 2017). In previous literature, whey, pea and casein proteins have been successfully conjugated to pectin and dextran polysaccharides. Pectin has shown enhanced properties (e.g., stability and emulsification) when conjugated to whey, soy, and potato proteins (Einhorn-Stoll et al., 2005; Li et al., 2021; Ma, Chen, et al., 2020; Ma, Hou, et al., 2020; Wefers et al., 2018). However, to our knowledge, the lubrication properties of such conjugated systems, particularly in plant-based proteins, have not been studied, and whether such conjugation improves the lubricity of plant proteins remains to be answered. If successful, the conjugates of Po and Pe can offer a promising ingredient-based approach toward sustainable plant-sourced food design with improved functional properties while maintaining the desired textural attributes.

Therefore, in this work, we report the first study on tribological and rheological properties of the Po and Pe mixture and conjugates. Our hypothesis was that Maillard glycation of Po with Pe will improve the lubricity of the former by virtue of viscosity modifying properties of Pe. We were particularly interested in understanding whether the changes in the tribology of the mixtures and their conjugates are mainly influenced by the protein or the polysaccharide component and how conjugation affects the above-mentioned properties versus their non-conjugated counterparts using a range of complementary techniques such as sizing, surface charge, and rheology.

TABLE 1 Nomenclature and composition of the samples.

Sample		Nomenclature	Potato protein (wt%)	Pectin (wt%)
Potato protein solutions		Po[0.5]	0.5	0
		Po[1]	1.0	0
		Po[1.25]	1.25	0
		Po[2.5]	2.5	0
		Po[5]	5.0	0
Pectin solutions		Pe[0.5]	0	0.5
		Pe[1]	0	1.0
		Pe[2.5]	0	2.5
		Pe[5]	0	5.0
Potato protein + Pectin mixtures		Po[0.5] + Pe[1]	0.5	1.0
		Po[1.25] + Pe[2.5]	1.25	2.5
		Po[2.5] + Pe[5]	2.5	5.0
		Po[0.5] + Pe[0.5]	0.5	0.5
		Po[2.5] + Pe[2.5]	2.5	2.5
Conjugated (Potato protein + Pectin) solutions	Po:Pe ratio: 1:2 w/w (1:0.2 mol/mol)	Conj$_{1:2}$(Po[0.5] + Pe[1])	0.5	1.0
		Conj$_{1:2}$(Po[1.25] + Pe[2.5])	1.25	2.5
		Conj$_{1:2}$(Po[2.5] + Pe[5])	2.5	5.0
	Po:Pe ratio: 1:1 w/w (1:0.1 mol/mol)	Conj$_{1:1}$(Po[0.5] + Pe[0.5])	0.5	0.5
		Conj$_{1:1}$(Po[2.5] + Pe[2.5])	2.5	2.5

MATERIALS AND METHODS

Materials

Po ($\sim$90% purity, Mw: $\sim$40 kDa, Kew et al., 2021), in a powdered form, was purchased from Sosa Ingredients SL (Barcelona, Spain). Pe powder (derived from citrus peel, dry content: 94%, methoxy groups on dry basis: 7.8%, Mw of nearly 400 kDa, Ma, Hou, et al., 2020), 4-(2-hydroxyethyl)-1-piperazineethanesulfonic acid (HEPES), sodium tetraborate, dithiothreitol and sodium dodecyl sulfate and sodium azide were purchased from Sigma Aldrich, (Dorset, UK). Potassium bromide (KBr, >99%) was purchased from Fisher Scientific (UK). An aqueous solution of 50 mM HEPES at pH 7.0, prepared in Milli-Q water with a resistivity of 18.2 MΩ cm at 25°C (Millipore Corp., Bedford, UK), was used as the buffer to prepare all the solutions used in this study. All chemicals were of analytical grade and were used with no further purification unless otherwise stated.

Methods

The composition of the samples tested in this study and their corresponding nomenclature are presented in Table 1. To obtain the solutions of Po, Pe, their mixtures and Maillard conjugates (without any added solvents), the Po and/or Pe powder were adjusted to the purity and gradually dispersed in 50 mM HEPES at defined dry-basis concentrations (Table 1) and were left to stir for at least 2 h at room temperature (25°C) using a magnetic stirrer. The pH of the solutions was measured and adjusted to pH 7.0 using an aqueous solution of 1.0 M sodium hydroxide (NaOH), if needed, immediately after the preparation of the solutions. Solutions of Po at concentrations of 0.5, 1, 1.25, 2.5, and 5 wt% (Po[0.5], Po[1], Po[1.25], Po[2.5], Po[5]), and Pe at the identical concentrations of 0.5, 1, 2.5, and 5 wt% (Pe[0.5], Pe[1], Pe[2.5], Pe[5]) were prepared to study the tribological and rheological properties of Po and Pe. The Po + Pe mixtures were prepared at two Po:Pe ratios of 1:1 w/w (1:0.1 mol/mol) and 1:2 w/w (1:0.2 mol/mol) to allow comparison of the influence of conjugation at the same Po:Pe ratios. The Po concentrations in the mixtures and conjugates were 0.5, 1.25, and 2.5 wt%. The tribological and rheological behavior of the mixtures at Po:Pe ratio of 1:1 w/w (i.e., Po[0.5] + Pe[0.5] and Po[2.5] + Pe[2.5]) was first assessed against: (1) the individual solutions of Po and Pe at the concentrations they exist in the mixture, (2) the total concentration of both biopolymers in the relevant mixture, and (3) the conjugate of the relevant mixture (i.e., Conj$_{1:1}$(Po[0.5] + Pe[0.5]) and Conj$_{1:1}$(Po[2.5] + Pe [2.5])). Next, we examined the influence of conjugation on the tribological and rheological behavior of the mixtures of Po and Pe at two Po:Pe ratios of 1:1 and 1:2 w/w (i.e., Po [0.5] + Pe[1], Po[1.25] + Pe[2.5], and Po[2.5] + Pe [5] vs. Conj$_{1:2}$(Po[0.5] + Pe[1]), Conj$_{1:2}$(Po[1.25] + Pe [2.5]), and Conj$_{1:2}$(Po[2.5] + Pe [5])). The purity of the protein and pectin in the respective powders was taken into account in preparing the solutions.

Preparation of conjugates

The conjugates of Po and Pe were produced through the Maillard reaction according to a process reported in a previous work by Soltanahmadi et al. (2022) with no additional solvent (i.e., dry conjugation). Briefly, the Po and Pe at 1:1 (8.33 g Po and 7.98 g Pe) or 1:2 (4.17 g Po and 7.98 g Pe) w/w ratios were mixed in 300 mL Milli-Q water at room temperature (25°C) for at least 2 h followed by a pH adjustment step to pH 10.0 to enhance the efficiency of the conjugation process (Araiza-Calahorra et al., 2020). The mixtures were then degassed using a Thinky mixer (Thinky ARE-250, Intertronics) at 2200 rpm for 3 min, placed in a freezer at −25°C for 24 h and freeze-dried (Freezone 2.5–50, Labconco) for at least 48 h. To promote the Maillard reaction the freeze-dried mixtures were placed in a glass desiccator equilibrated with a saturated solution of KBr in Milli-Q water (relative humidity of ~80% at 25°C) and heat treated for 5 days in a preheated oven at 60°C. The Maillard reaction parameters were adopted based on previous works (Araiza-Calahorra et al., 2020; Soltanahmadi et al., 2022) and pilot trials (data not shown) with shorter time intervals of reaction (i.e., 24 and 48 h yielded small degree of conjugation). The produced conjugates of Po and Pe were stored in a dry desiccator before and after each use. The freeze-dried conjugates were ground using a pestle and mortar and dispersed in HEPES buffer to prepare the conjugated solutions at the defined concentrations (Table 1). The pH of the conjugated solutions was adjusted to pH 7.0 before further analysis.

Determination of the degree of conjugation

The degree of conjugation (DC) was measured using the o-phthalaldehyde (OPA) assay, which can detect the content of free amino acids in the protein (i.e., Po) before and after conjugation with Pe (Fan et al., 2018). The assay was adapted from a previous study (Nielsen et al., 2001). Briefly, 3.81 g sodium tetraborate, 0.088 g dithiothreitol and 0.1 g sodium dodecyl sulfate were dissolved in 80 mL Milli-Q water and mixed with 0.080 g OPA, pre-dissolved in 2 mL ethanol, followed by making up the volume to 100 mL using Milli-Q water. 1 mg/mL of samples were prepared by mixing the conjugated powder in Milli-Q water and filtered through syringe filters (1.0 μm, PES, GE Life Sciences Whatman). For the OPA analysis, 3 mL OPA reagent was added into a disposable cuvette, followed by the addition of 150 μL of the 1 mg/mL conjugated solution and left to rest at room temperature (25°C) for 10 min. The UV absorbance at 340 nm was measured with a UV–VIS spectrophotometer (Specord 210 PLUS, Analytik Jena, Germany). The standard curve was plotted by detecting the absorbance of a series of L-leucine standard solutions (0–200 μM). The DC% was calculated using the Equation 1:

$$\mathrm{DC\%} = \left(\frac{C_{\mathrm{unconjugated}} - C_{\mathrm{conjugated}}}{C_{\mathrm{unconjugated}}}\right) \times 100 \qquad (1)$$

where, $C_{\mathrm{unconjugated}}$ is the concentration of free amino acids in the unconjugated Po-Pe samples that is, before the Maillard conjugation reaction; $C_{\mathrm{conjugated}}$ is the concentration of conjugated Po-Pe samples with various Po:Pe weight ratios.

Particle size and zeta-potential

The particle size and zeta-potential (ζ-potential) of the samples were measured at 25°C using a Zetasizer (Ultra Zetasizer, Malvern Instruments Ltd., Worcestershire, UK). The particle size (d_H) was measured by dynamic light scattering (DLS). The refractive indices (RI) of 1.33, 1.45, 1.54 for the aqueous solvent, protein-containing dispersions and pectin dispersions were used, respectively. Sample solutions were diluted ×50 and 100 (v/v) using 50 mM HEPES (pH 7.0) for size and ζ-potential measurements, respectively, followed by sonication for at least 15 min prior to each measurement.

Apparent viscosity

The flow behavior of samples was characterized using a controlled-stress rheometer (Kinexus, Malvern Instruments Ltd., Worcestershire, UK) equipped with a plate-on-plate geometry (PL 65). The gap was fixed at 0.5 mm, and the apparent viscosity of solutions was measured as a function of increasing shear rate from 0.1 to 2000 s^{-1} (five readings per decade) at 37°C to replicate the oral physiological temperature. About 1 mL of the sample was loaded onto the bottom plate geometry ensuring the absence of any air bubbles. The solution was allowed to rest 5 min on the bottom geometry to reach an equilibrium state before acquiring the viscosity data.

Tribology

The tribological performance of the samples was measured using a Mini-Traction Machine (MTM, PCS Instruments, UK) at 37°C. A ball-on-disk configuration was used with polydimethylsiloxane (PDMS) specimens (PCS Instruments, UK). The diameter of the ball and disc was 19 and 46 mm, respectively. The friction coefficient (μ) results were recorded as a function of increasing entrainment speed (u, u: 1–3000 mm/s), and under 2.0 N normal load (equivalent to a maximum Hertzian contact pressure of ~200 kPa, Sarkar et al., 2019) and slide-to-roll ratio (SRR) of 50%. Before each test, the PDMS specimens were thoroughly cleaned by sonication steps in sequence with an aqueous solution of sodium dodecyl sulfate, isopropanol alcohol, and finally Milli-Q water to remove any traces of contamination. Each solution was tested in triplicate using three separate pairs of PDMS specimens.

Statistical analyses

The mean and standard deviation (SD) data were calculated from at least three readings on triplicate experiments using Origin 2018. One-way ANOVA (Tukey test) was conducted using SPSS statistical software (version 27) to identify the significant differences between the tested samples. A significant difference was recognized as $p < 0.05$.

RESULTS AND DISCUSSION

First, we examined the DC% of the Po-Pe conjugates and investigated their physicochemical properties in order to understand whether differences (if any) versus the individual protein, polysaccharide solution or mixture will influence their rheological and tribological properties.

Degree of conjugation (DC%)

The DC% was increased from 19.7 ± 1.9% at the Po:Pe ratio of 1:1 w/w to 32.8 ± 1.7% at the Po:Pe ratio of 1:2 w/w prepared under the same processing conditions. With an enhanced availability of sugar (carbonyl) groups for conjugation during the Maillard reaction, a higher DC is expected corroborating our observation. This is in agreement with the results previously reported by Araiza-Calahorra et al. (2020) and Yao et al. (2022) for other protein-polysaccharide-based conjugates.

Particle size and zeta-potential

The surface-charge characteristics and hydrodynamic diameter (d_H) of biopolymers play an important role in understanding the behavior of biopolymers at a certain pH and ionic condition. Table 2 shows the ζ-potential values, d_H and polydispersity index (PDI) for Po solutions, Pe solutions, their mixtures and conjugates. Specifically, all samples in the study were negatively charged at pH 7.0. In the case of Po solutions, ranging from 0.5 to 5 wt%, the average ζ-potential value insignificantly varied between −16 and −20 ($p > 0.05$) at the neutral pH condition. This is in agreement with the previous findings of Kew et al. (2021) and can be attributed to the isoelectric point (pI) of Po, which has been reported as pH 4.5–5.0 (Schmidt et al., 2019).

All tested Pe solutions were negatively charged, with ζ-potential values ranging between −18 and −30 mV at pH 7.0 (Table 2) depending upon the concentration. A higher degree of negatively charged carboxylic groups in Pe at higher concentration can shift the ζ-potentials to more negative values ($p < 0.05$ except for Pe[1] and Pe[2.5]). These groups are known to ionize at pH levels above the pKa of Pe (≈3.4), presenting negative ζ-potentials (Sriamornsak et al., 2010). The number of carboxyl groups in pectin largely depends on the galacturonic acid content and the various degree of esterification available commercially. These compositional differences influence the ζ-potential, which might be responsible for the difference in results between studies (Lan et al., 2020).

Upon mixing Po and Pe, the net surface charges of all studied mixtures shifted toward more negative values (relatively large variations ranging from −24 to −38 mV) than their corresponding individual Po solutions ($p < 0.05$) (Table 2). A similar trend has been seen in the case of pea protein and pectin mixtures (Lan et al., 2020). This can be attributed to the increased number of negatively charged carboxyl groups in the mixtures with the addition of Pe to the Po solutions. It is noteworthy that the ζ-potential values of mixtures were linked to the applied Po:Pe weight ratio (1:1 or 1:2 w/w in this study), which was also reported in pectin and mucin (a biological family of glycosylated proteins) mixtures by Sriamornsak et al. (2010). Proteins are polyionic and thus even if the net ζ-potential is negative, they still have some positively-charged groups. Therefore, electrostatic interactions between proteins and polysaccharides in mixtures can bring about complexation impacting ζ-potential results (Lutz et al., 2009). A hypothesis here to explain the rise in negative ζ-potentials is the weak ionic interactions between some positively-charged moieties of Po fragments and negatively-charged Pe, which mask the originally positive charges, resulting in overall negative charge on the surface (Lutz et al., 2009).

The Po-Pe conjugates displayed almost identical ζ-potential values (close to −35 mV, Table 2) irrespective of the concentration and degree of conjugation (DC) ($p > 0.05$). Therefore, a stable structure can be inferred as a result of the Maillard-type interactions between Po and Pe as compared to the corresponding mixtures. Most of the conjugates analyzed in this study were found to be more negatively-charged compared to their mixture counterparts or individual biopolymer solutions ($p < 0.05$) (Table 2). This might be due to some changes in the secondary structure (i.e., denaturation) of proteins in the conjugates increasing the mobility

TABLE 2 Mean ζ-potential values, hydrodynamic diameter (d_H) and polydispersity index (PDI) of proteins, polysaccharides, mixtures, and conjugates.

Sample	ζ-potential (mV)	d_H (nm)	PDI
Po[0.5]	$-16^{g} \pm 2$	$31^{h} \pm 1$	0.59 ± 0.11
Po[1]	$-19^{g} \pm 1$	$32^{h} \pm 1$	0.49 ± 0.03
Po[1.25]	$-17^{g} \pm 1$	$33^{h} \pm 1$	0.50 ± 0.04
Po[2.5]	$-20^{fg} \pm 1$	$33^{h} \pm 1$	0.47 ± 0.01
Po[5]	$-20^{fg} \pm 1$	$36^{h} \pm 1$	0.43 ± 0.01
Pe[0.5]	$-18^{g} \pm 1$	$632^{g} \pm 22$	0.49 ± 0.03
Pe[1]	$-25^{de} \pm 1$	$669^{g} \pm 31$	0.47 ± 0.06
Pe[2.5]	$-24^{ef} \pm 1$	$776^{g} \pm 17$	0.34 ± 0.04
Pe[5]	$-30^{bc} \pm 1$	$1470^{e} \pm 43$	0.23 ± 0.03
Po[0.5] + Pe[0.5]	$-24^{ef} \pm 2$	$779^{fg} \pm 114$	0.63 ± 0.07
Po[0.5] + Pe[1]	$-29^{cd} \pm 1$	$796^{fg} \pm 99$	0.69 ± 0.05
Po[1.25] + Pe[2.5]	$-35^{b} \pm 2$	$1310^{ef} \pm 73$	0.46 ± 0.11
Po[2.5] + Pe[2.5]	$-25^{de} \pm 1$	$2550^{d} \pm 206$	1.15 ± 0.28
Po[2.5] + Pe[5]	$-38^{a} \pm 1$	$1340^{e} \pm 71$	0.54 ± 0.11
$\text{Conj}_{1:2}$(Po[0.5] + Pe[1])	$-36^{a} \pm 1$	$4100^{a} \pm 372$	0.47 ± 0.05
$\text{Conj}_{1:2}$(Po[1.25] + Pe[2.5])	$-35^{a} \pm 1$	$3468^{b} \pm 406$	0.29 ± 0.18
$\text{Conj}_{1:2}$(Po[2.5] + Pe[5])	$-35^{a} \pm 1$	$3230^{bc} \pm 582$	0.42 ± 0.07
$\text{Conj}_{1:1}$(Po[0.5] + Pe[0.5])	$-34^{ab} \pm 2$	$2380^{d} \pm 211$	0.52 ± 0.32
$\text{Conj}_{1:1}$(Po[2.5] + Pe[2.5])	$-36^{a} \pm 2$	$2820^{cd} \pm 243$	1.14 ± 0.16

Note: Values are presented as means ± standard deviations (SD). Subscript letters after mean values are used to indicate the significant difference between tested samples. Values with completely different letters are significantly different ($p < 0.05$).

and exposure of a few previously hidden charged groups in addition to the impact of grafting of Pe chains in the conjugates (Ma et al., 2022).

Po solutions showed a consistent mean d_H ranging from 31 to 36 nm ($p > 0.05$), which is similar to the observations previously reported by Kew et al. (2021) (Table 2). A broad size distribution for the Po solutions, together with relatively high PDI (around 0.43–0.59) suggested polydispersity of potato protein moieties. The high molecular weight of Pe and its branched nature led to d_H values between 632 and 1470 nm which were significantly larger ($p < 0.05$) than those of Po solutions. Measuring Pe, mixtures with Po and conjugates with DLS should be taken with caution as these are not spherical particles and all the data fitting for calculating d_H assumes the particle to be spherical. Except for Po[2.5] + Pe[5], the mixtures of Po and Pe demonstrated larger average d_H values than the corresponding Pe solutions, suggesting interactions between Po and Pe (i.e., hydrogen bonds, van der Waals association) (Pang et al., 2023). The effect of concentration on ζ-potential and d_H values of the Pe solutions and mixtures, as opposed to concentration independency of the Po solutions, suggested that intermolecular interactions were not fully broken down even after the dilution. This can be attributed to the significantly higher molecular weight of Pe as compared to that of Po.

The conjugation resulted in the most significant increase in d_H values (2380–4100 nm, $p < 0.05$ compared to the corresponding mixtures), which corroborates the hypothesis that the increased mobility brought about the more negative ζ-potential values of conjugates compared to the associated mixtures and the biopolymers. Further, formation of Pe-wrapped particles with sizes of a few thousands of nanometers (Table 2) can be envisaged for the conjugates driven by the covalent linkage between Po and Pe and also the freeze-drying process as observed for other protein-polysaccharide conjugates (e.g., corn fiber gum–milk protein conjugates; pectin-pea protein conjugates) in the literature (Tamnak et al., 2016; Yadav et al., 2012).

Rheological and lubrication behavior of individual Po or Pe solutions

Flow behavior of Po and Pe

The apparent viscosity (η) – shear rate ($\dot{\gamma}$) graphs for the Po and Pe solutions are shown in Figure 1a,b, respectively. The η values for the Po solutions at high shear rates ($\dot{\gamma} = 1000\ \text{s}^{-1}$) were similar ($p > 0.05$) with negligible concentration dependence as also shown in the size data (Table 2). Similar to previous

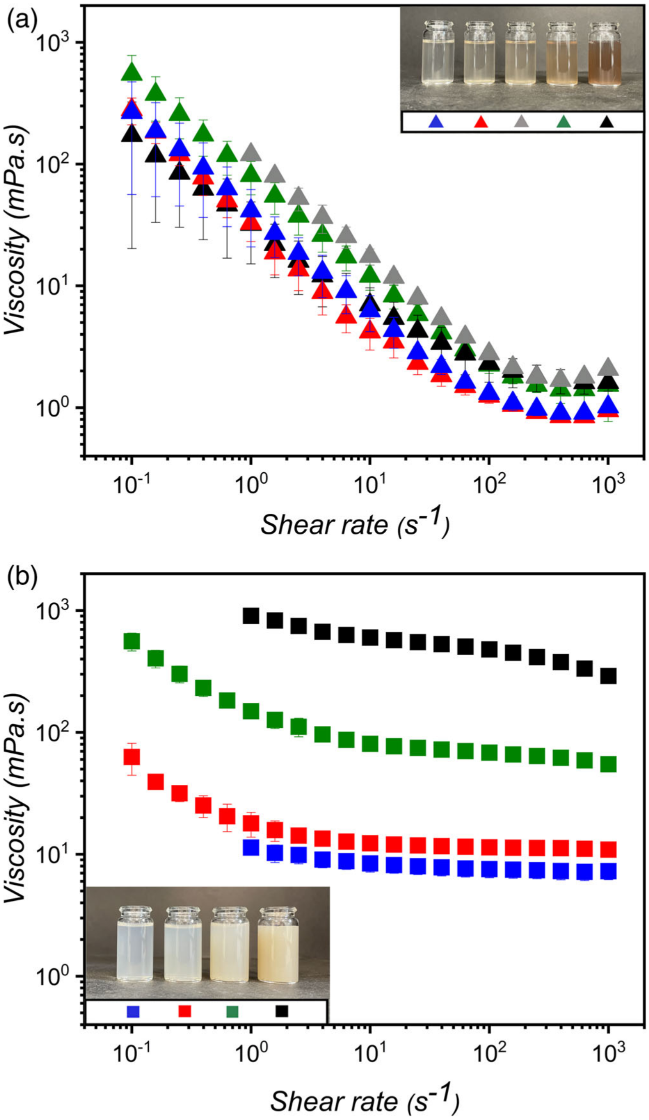

FIGURE 1 Viscosity (η) of (a) Po solutions: Po[0.5] ▲, Po[1] ▲, Po[1.25] ▲, Po[2.5] ▲, Po[5] ▲, and (b) Pe solutions: Pe[0.5] ■, Pe[1] ■, Po[2.5] ■, Po[5] ■ as a function of shear rate ($\dot{\gamma}$), respectively. Data represent means and standard deviations for at least three measurements on two independent samples ($n = 3 \times 2$). The visual images of Po and Pe solutions at pH 7, 25°C were shown, in which the biopolymer concentration increases from left to right.

findings by Kew et al. (2021), the $\eta - \dot{\gamma}$ graphs for Po solutions showed shear-thinning behavior with the η values showing two orders of magnitude decay across the measured $\dot{\gamma}$ (Figure 1a). Generally plant proteins tend to aggregate as shown by the high PDI in Table 2 and the breakup of such aggregates of Po and alignment in direction of flow was most likely responsible for such pseudo-plastic behavior (Soltanahmadi et al., 2022).

In contrast, $\eta - \dot{\gamma}$ graphs for Pe solutions showed a slight shear-thinning character as a function of the shear window tested in this study (Figure 1b). A concentration-dependent behavior was observed for η of Pe solutions that is, higher η values were obtained with increasing concentration. For instance, the mean η at $\dot{\gamma} = 1000\ s^{-1}$ increased by nearly four folds for Pe [5] (290.4 mPa.s) as compared to that for Pe[0.5] (7.3 mPa.s) (Figure 1b), which is also in line with occupying more hydrodynamic volume (see higher d_H in Pe [5] vs. Pe[0.5] in Table 2). The η of Pe solutions at $\dot{\gamma} = 1000\ s^{-1}$ were considerably higher as compared to those of Po solutions at the corresponding concentration (Figure 1a, $p < 0.05$). At low shear rates ($\dot{\gamma} < 1\ s^{-1}$), a similar non-Newtonian behavior for a Pe solution was observed by Tiwari et al. (2010). This shear-thinning might be attributed to the breakdown of weak aggregates in the Pe solutions (Li et al., 2013). The rather lesser decrease of η for dilute Pe solutions has been reported with increasing $\dot{\gamma}$ (until a certain shear rate) due to weaker interactions between Pe chains, whereas interpenetration between polymer chains and slower chain alignment is expected to occur in concentrated solutions (Morris et al., 1984). The latter structural conformation could be disturbed by the flow stream, leading to extended shear thinning (Inglett et al., 2015).

Lubrication behavior of Po and Pe

The coefficient of friction (μ) results as a function of entrainment speed (u) for Po and Pe solutions are shown in Figure $2a_1,b_1$, respectively. Po solutions at all concentrations exhibited all four lubrication regimes of boundary, mixed, elasto-hydrodynamic (EHL) and hydrodynamic (HDL) across the measured u. At higher Po concentrations, lower μ values were observed at the boundary and mixed lubrication regimes, which were in close agreement with the previous findings of Kew et al. (2021). The boundary μ values were 0.85, 0.76, 0.55, 0.44, and 0.29 for Po[0.5], Po[1], Po[1.25], Po [2.5], and Po[5], respectively, showing a significant difference between Po[5] and Po[0.5] ($p < 0.05$) (Figure $2a_1$). The onset of EHL regime (u_{EHL}) took place at similar u values for all Po solutions, except for Po[5], which showed a shift to a lower u value. The μ at the u_{EHL} (i.e., the lowest μ value: μ_{EHL}) was $\sim 2 \times 10^{-3}$ for all Po solutions ($p > 0.05$).

Pe solutions at the low concentrations of Pe[0.5] and Pe [1] almost reached a boundary regime and showed similar boundary μ of 0.45, which was ~44% lower than that of Po[0.5] and Po[1], respectively ($p < 0.05$). Lower u_{EHL} values were observed at higher concentrations of Pe which results from increased viscosity of solutions prompting viscous lubricity (Sarkar et al., 2021; Selway et al., 2017). While Pe[2.5] mostly remained at the mixed lubrication regime at $3 \times 10^{-3} < u < 8 \times 10^{-2}\ m.s^{-1}$, Pe[5] did not enter into a mixed lubrication regime at the measured u range. The Pe[2.5] solution appeared to nearly level off at

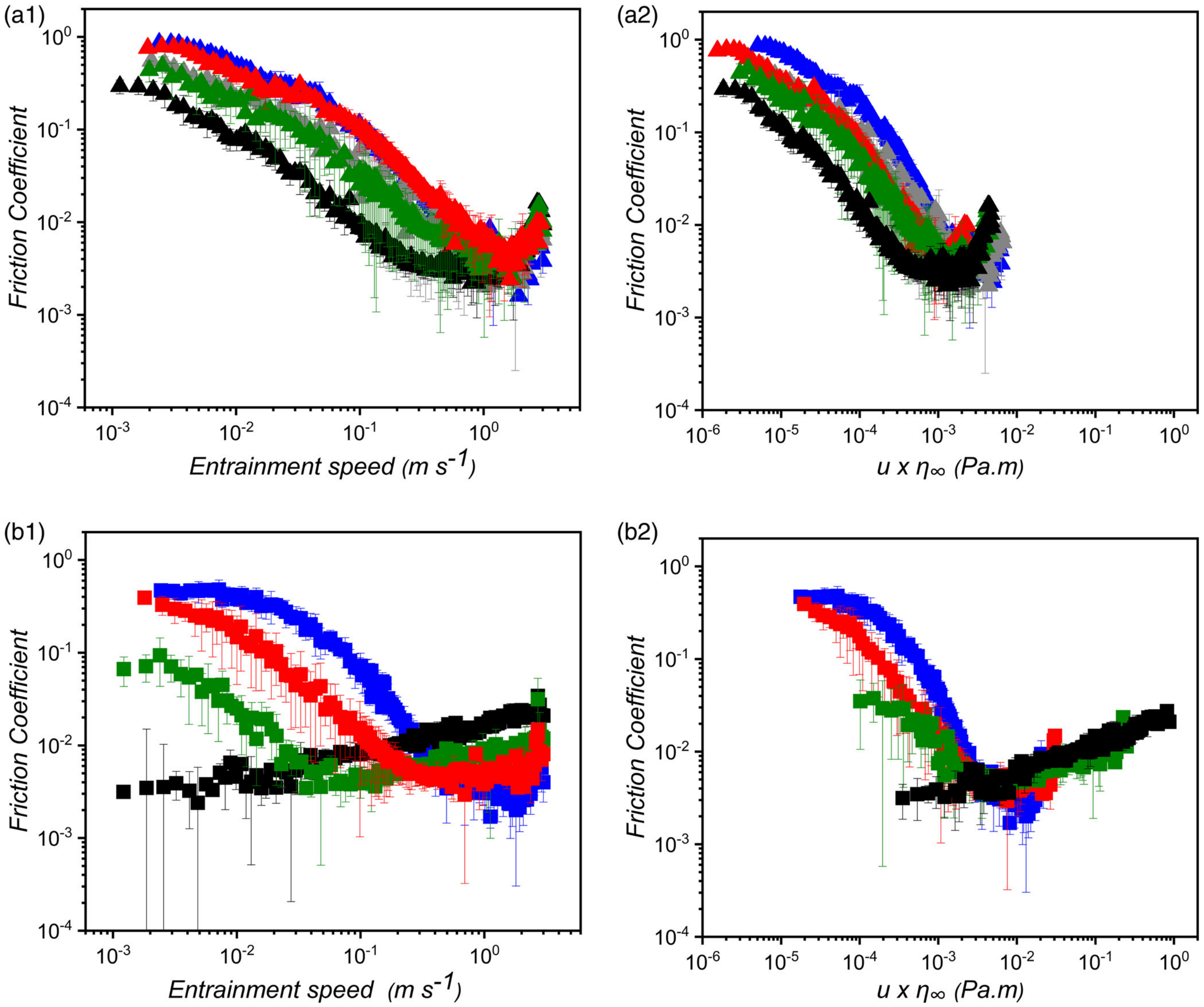

FIGURE 2 Friction coefficient (μ) results for (a_1 and a_2) potato protein solutions Po[0.5] ▲, Po[1] ▲, Po[1.25] ▲, Po[2.5] ▲, Po[5] ▲, and (b_1 and b_2) pectin solutions Pe[0.5] ■, Pe[1] ■, Pe[2.5] ■, Pe[5] ■ as a function of (a_1 and b_1) entrainment speed, u or (a_2 and b_2) the product of entrainment speed and high-shear rate viscosity, $u \times \eta_\infty$. Data represent means and standard deviations for at least two independent samples ($n = 3 \times 2$).

$u = 3 \times 10^{-3}$ suggesting a boundary μ of $\sim 8 \times 10^{-2}$; 85% lower than that of Po[2.5] ($p < 0.05$).

Figure 2a₂,b₂ show the $\mu - u \times \eta_\infty$ graphs for Po and Pe solutions, respectively, to disintegrate the influence of the bulk viscosity of solutions from their surface effect (e.g., adsorption) on the lubrication performance (de Vicente et al., 2005; Sarkar et al., 2021; Selway et al., 2017). The limiting high-shear viscosity (where the $\eta - \dot{\gamma}$ plateaued; η_∞) for each solution was determined and used to obtain $\mu - u \times \eta_\infty$ graphs. For the Po and Pe solutions η at $\dot{\gamma} = 1000\ \mathrm{s}^{-1}$ was assigned as the η_∞.

Po solutions at higher concentrations showed lower μ values at the mixed and boundary lubrication regime (Figure 2a₂) suggesting the surface activity of Po plays a role in friction reduction when surfaces are in close proximity. This can be attributed to the surface adsorption of Po on PDMS surfaces as previously evidenced using quartz crystal microbalance with dissipation monitoring (QCM-D) (Kew et al., 2021) and effective wetting of the contact interfaces by Po molecules reducing the rate of fluid squeeze-out from the contact interface (Selway et al., 2017).

As the concentration of Pe increased (Figure 2b₂), lower μ values at the mixed and the boundary regimes and a shift in u_{EHL} to lower u values were observed. Such behavior was attributed to the surface adsorption of Pe (Stokes et al., 2011) and the viscous forces (higher η) which hinder the squeeze-out and de-wetting of the Pe solution from the contact interfaces (Selway et al., 2017; Soltanahmadi et al., 2022).

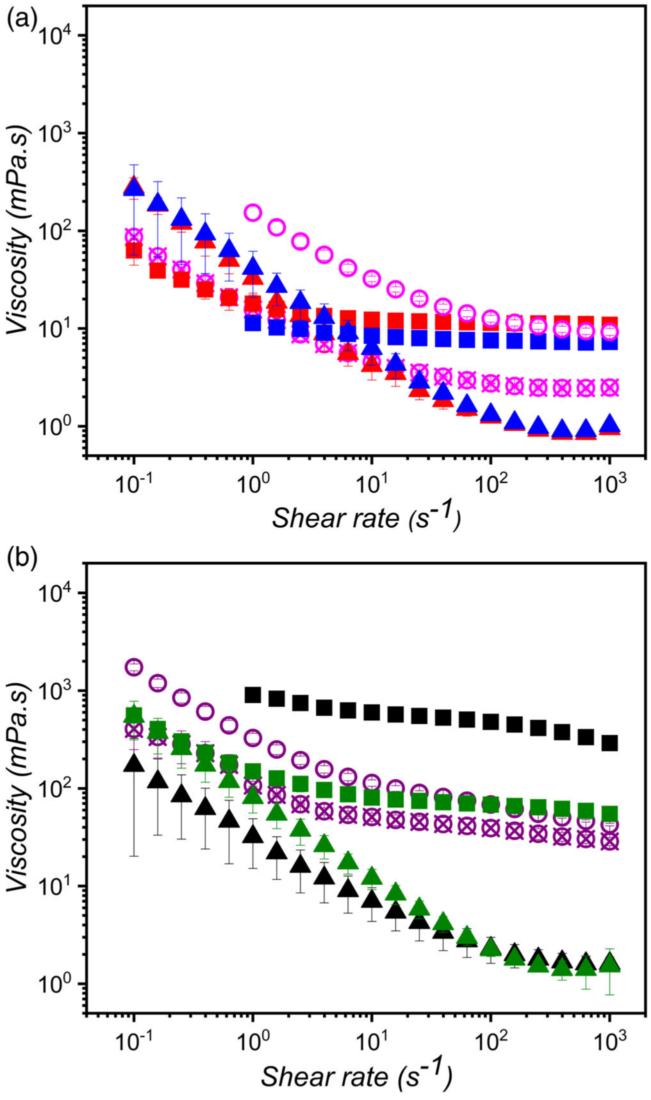

FIGURE 3 Viscosity (η) – shear rate ($\dot{\gamma}$) graphs for biopolymer mixtures of Po and Pe, and their conjugated solutions at a Po:Pe ratio of 1:1 w/w at a total biopolymer concentration of (a) 1.0 wt% (Po[0.5] + Pe[0.5] ○, Conj$_{1:1}$(Po[0.5] + Pe[0.5]) ⊠) and (b) 5.0 wt% (Po[2.5] + Pe[2.5] ○, Conj$_{1:1}$(Po[2.5] + Pe[2. 5]) ⊠. $\eta - \dot{\gamma}$ graphs for Po solutions (Po[0.5] ▲, Po[1] ▲, Po[2.5] ▲, Po[5] ▲) and Pe solutions (Pe [0.5] ■, Pe[1] ■, Pe[2.5] ■, Pe[5] ■) are shown for comparison purposes. Data represent means and standard deviations for three measurements for at least two independent samples ($n = 3 \times 2$).

Comparison of rheological and lubrication behavior of mixtures and conjugates versus individual biopolymer solutions

Next, we studied the unconjugated mixtures and conjugated solutions of Po and Pe when mixed at the same ratio (i.e., 1:1) at low (0.5 wt%) and high (2.5 wt%) Po or Pe concentrations and compared the mixtures against the individual biopolymer solutions (i.e., Po [0.5], Po[1], Po[2.5], Po[5], Pe[0.5], Pe[1], Pe[2.5], and Pe[5]). The question here was that in a mixture of Po and Pe blended at the same concentration, which component has a more pronounced influence on the rheological and lubrication behavior of the mixture. Whether the flow or lubrication is a factor of the total concentration of biopolymers or the concentration of each component in the mixture, and how conjugation influences the above-mentioned parameters were examined.

Comparison of rheological behavior of Po and Pe, their mixtures and conjugates

Upon addition of Po to Pe, the shear-thinning behavior of Po was more pronounced in the mixtures (and conjugated mixtures, Figure 3a,b). This corroborates with the increased hydrodynamic size of the mixtures and conjugates upon addition of Pe (Table 2). At both concentrations and high shear rates ($\dot{\gamma} > 100$ s^{-1}), the η of mixtures resembled either of their individual components (Po or Pe) at the concentrations they exist in the mixtures rather than the total concentration of the biopolymers (C%: Po + Pe). At the low concentration (Figure 3a) and relatively high shear rates ($\dot{\gamma} > 50$ s^{-1}), η values of the mixture (Po[0.5] + Pe[0.5]) and the conjugate (Conj$_{1:1}$(Po[0.5] + Pe[0.5])) were close to those of the Pe component (Pe[0.5]) and the Po component (Po[0.5]), respectively. This suggests that the aggregates formed in the mixture or conjugates at low biopolymer concentration shown by large hydrodynamic sizes (Table 2) were rather easy to be broken down by shear rates that can occur in mouth. At the high concentration (Figure 3b) and high shear rates, η values of both the mixture (Po[2.5] + Pe[2.5]) and the conjugate (Conj$_{1:1}$(Po[2.5] + Pe[2.5])) were comparable to those of the Pe component (Pe[2.5]) which were significantly higher than η of Po[2.5]. According to the above, it can be inferred that Pe dominated the flow behavior of mixtures and conjugated mixtures at $\dot{\gamma} > 100$ s^{-1}, especially at the high concentration. This is in line with the rheological properties of other biopolymer mixtures studied previously (You et al., 2021, 2023).

The Maillard conjugation was found to reduce η values across the measured $\dot{\gamma}$ (Figure 3a,b), with a more pronounced effect at lower concentrations (Figure 3a). The η_∞ for Conj$_{1:1}$(Po[0.5] + Pe[0.5]) and Conj$_{1:1}$(Po[2.5] + Pe[2.5]) was ~2.49 and 28.64 mPa. s, respectively, indicating a 73% and 33% reduction following conjugation for the former and latter. Al-Hakkak and Al-Hakkak (2010) observed a similar conjugation effect on η for pectin-egg white protein conjugates. This effect could result from the exclusion of the heat-induced insoluble high-molecular weight protein fragments from taking part in the viscous flow of the conjugated solutions (Al-Hakkak & Al-Hakkak, 2010). Furthermore, the reduction in η as a result of conjugation could be attributed to the decreased molecular weight of Pe during Maillard reaction

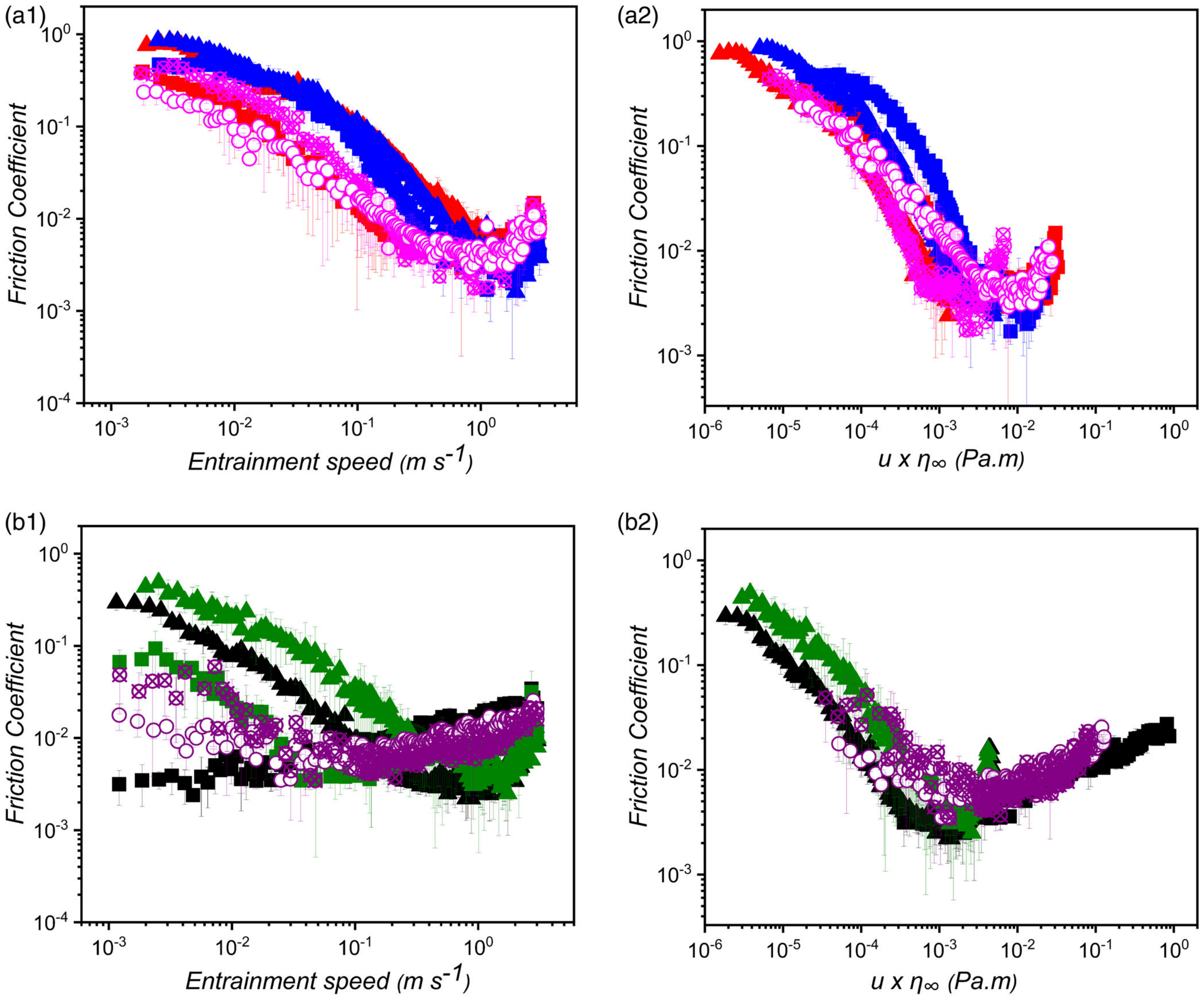

FIGURE 4 Friction coefficient (μ) results for biopolymer mixtures of potato protein and pectin, and their conjugated solutions at a potato protein to pectin ratio of 1: 1 w/w at a total biopolymer concentration of (a_1 and a_2) 1.0 wt% (Po[0.5] + Pe[0.5] ○, Conj$_{1:1}$(Po[0.5] + Pe[0.5]) ⊠) and (b) 5.0 wt% and (b_1 and b_2) 5.0 wt% (Po[2.5] + Pe[2.5] ○, Conj$_{1:1}$(Po[2.5] + Pe[2. 5]) ⊠). The μ results are presented as a function of (a_1 and b_1) entrainment speed, u or (a_2 and b_2) the product of entrainment speed and high-shear rate viscosity, $u \times \eta_\infty$. The μ results for potato protein solutions (Po[0.5] ▲, Po[1] ▲, Po[2.5] ▲, Po[5] ▲) and Pe solutions (Pe[0.5] ■, Pe[1] ■, Pe[2.5] ■, Pe[5] ■) are shown for comparisons purposes. Data represent means and standard deviations for at least three measurements on two independent samples ($n = 3 \times 2$).

(Wang et al., 2022) or strong intermolecular repulsive interactions between Po and Pe during Maillard reaction. The latter also can be observed by the shift in the ζ-potential to more negative values (Table 2), this could diminish the protein–protein aggregation in Po leading to lower viscosity (Castellanos et al., 2014).

Comparison of the lubrication behavior of Po and Pe, their mixtures and conjugates

Figure 4 shows the $\mu - u$ graphs of the mixtures at Pe or Po concentration of 0.5 wt% (i.e., Po[0.5] + Pe[0.5], Figure 4a_1) and 2.5 wt% (i.e., Po[2.5] + Pe[2.5], Figure 4b_1), together with the associated Po or Pe solutions and the conjugated mixtures.

At the boundary lubrication regime, the Po[0.5] + Pe[0.5] mixture and its conjugate (i.e., Conj$_{1:1}$(Po[0.5] + Pe[0.5])) showed comparable μ values, similar to those of Pe[0.5] and Pe[1] ($p > 0.05$) and significantly lower than those of Po[0.5] and Po[1] ($p < 0.05$; Figure 4a_1). This implies that the adsorption of Pe on the PDMS surfaces dominates the boundary lubricity of the mixtures and enhances the lubricity of the Po solution. In the mixed regime, the Po[0.5] + Pe[0.5] mixture showed lower μ values as compared to Pe[0.5], Po [0.5], and Po[1], but higher μ values than Pe [1] ($p < 0.05$). This observation corroborates the high-shear flow behavior of Po[0.5] + Pe[0.5] (Figure 3a) which showed η values between Pe[0.5] and Pe [1] and indicates the dominant influence of viscous lubricity.

When Po and Pe were mixed at a higher concentration (i.e., Po[2.5] + Pe[2.5]), the $\mu - u$ did not plateau at the lowest measured u and showed considerably lower μ values at $u < 5 \times 10^{-2}$ m.s^{-1} as compared to Pe[2.5], Po[2.5], and Po[5], but higher than Pe[5] ($p < 0.05$) (Figure 4b$_1$). Considering slightly lower η values of the mixture (at high shear rates) relative to Pe[2.5] (Figure 3b), it can be inferred that the interactions between Po and Pe provide more effective lubricity at least at the mixed lubrication regime. Similar to Po[0.5] + Pe[0.5], the dominant component of Po[2.5] + Pe [2.5], to reduce μ is Pe bringing about significantly lower μ as compared to Po[2.5] and even Po[5] (i.e., the total concentration of the biopolymers). The conjugation appeared to increase μ at the mixed regime (Figure 4a$_1$,b$_1$), which can be expected considering the lower η_∞ of conjugates compared to their associated mixtures (Figure 3a,b). Nevertheless, both mixtures and conjugates appeared to show significantly lower μ values versus Po[2.5] and Po[5] at $u < 10^{-1}$ m.s^{-1} ($p < 0.05$) with conjugates forming a stable negatively-charged structure. Further, when the μ of the conjugates were considered, a higher extent of μ reduction was observed when compared to Po[2.5] than to Pe [2.5]. This indicates that conjugation of Pe to Po generates a protein-rich stable structure with improved lubrication properties.

Figure 4a$_2$,b$_2$ show the $\mu - u \times \eta_\infty$ graphs for the mixtures and their conjugates at [Pe or Po]: 0.5 and 2.5 wt%, respectively. Figure 4a$_2$,b$_2$ corroborate the findings of Figure 4a$_1$,b$_1$ suggesting the dominant influence of viscous behavior of Pe on the μ of the Po + Pe mixtures and conjugates at the boundary and mixed regimes.

Influence of Po:Pe ratio on the flow and lubrication behavior of mixtures and conjugates

We observed a 67% increase in DC% was observed when the Po:Pe concentration was halved. Hence, it was pertinent to ask whether a higher degree of conjugation can influence the flow and lubrication behavior of mixtures.

The influence of Po:Pe ratio on the rheological behavior of Po-Pe conjugates

Figure 5a,b compare the influence of Po:Pe on the flow behavior of the conjugates. Similar to Po:Pe at the ratio of 1:1 w/w (Figure 5b), the conjugation reduced η of the corresponding mixtures across the examined concentrations

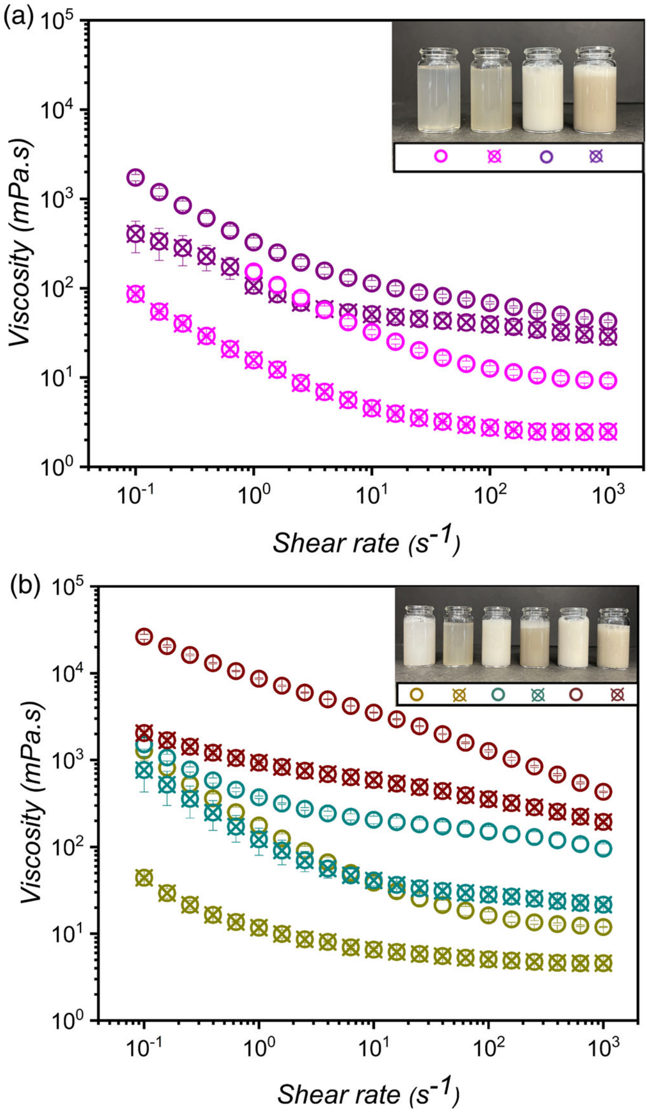

FIGURE 5 Viscosity (η) – shear rate ($\dot{\gamma}$) graphs for biopolymer mixtures of Po and Pe, and their conjugated solutions at a Po to Pe ratio of (a) 1: 1 w/w (Po[0.5] + Pe[0.5] ○, Conj$_{1:1}$(Po[0.5] + Pe[0.5]) ⊗, Po[2.5] + Pe[2.5] ○, Conj$_{1:1}$(Po[2.5] + Pe[2. 5]) ⊗) and (b) 1: 2 w/w (Po[0.5] + Pe[1] ○, Conj$_{1:2}$(Po[0.5] + Pe[1]) ⊗, Po[1.25] + Pe[2.5] ○, Conj$_{1:2}$(Po[1.25] + Pe[2. 5]) ⊗, Po[2.5] + Pe[5] ○, Conj$_{1:2}$(Po[2.5] + Pe[5]) ⊗). Data represent means and standard deviations for at least two independent samples ($n = 3 \times 2$). The visual images of Po and Pe mixtures and conjugates at pH 7, 25°C were shown.

and $\dot{\gamma}$ at Po:Pe of 1:2 w/w (Figure 5a), with a higher effect at the lower $\dot{\gamma}$ values. No monotonic correlation was observed between the concentration and reduction in η following the conjugation (Figure 5).

All dispersions presented in Figure 5 showed prominent shear-thinning behavior as might be expected from their higher hydrodynamic size and PDI (Table 2), at least at $\dot{\gamma} < 10$ s^{-1}, after which solutions with a Pe concentration of 0.5, 1, or 2.5 wt% reached a plateau as $\dot{\gamma}$ increased. The increased concentration of Pe was found to be the most pronounced factor to enhance η of the solutions implying a beneficial viscous lubricity

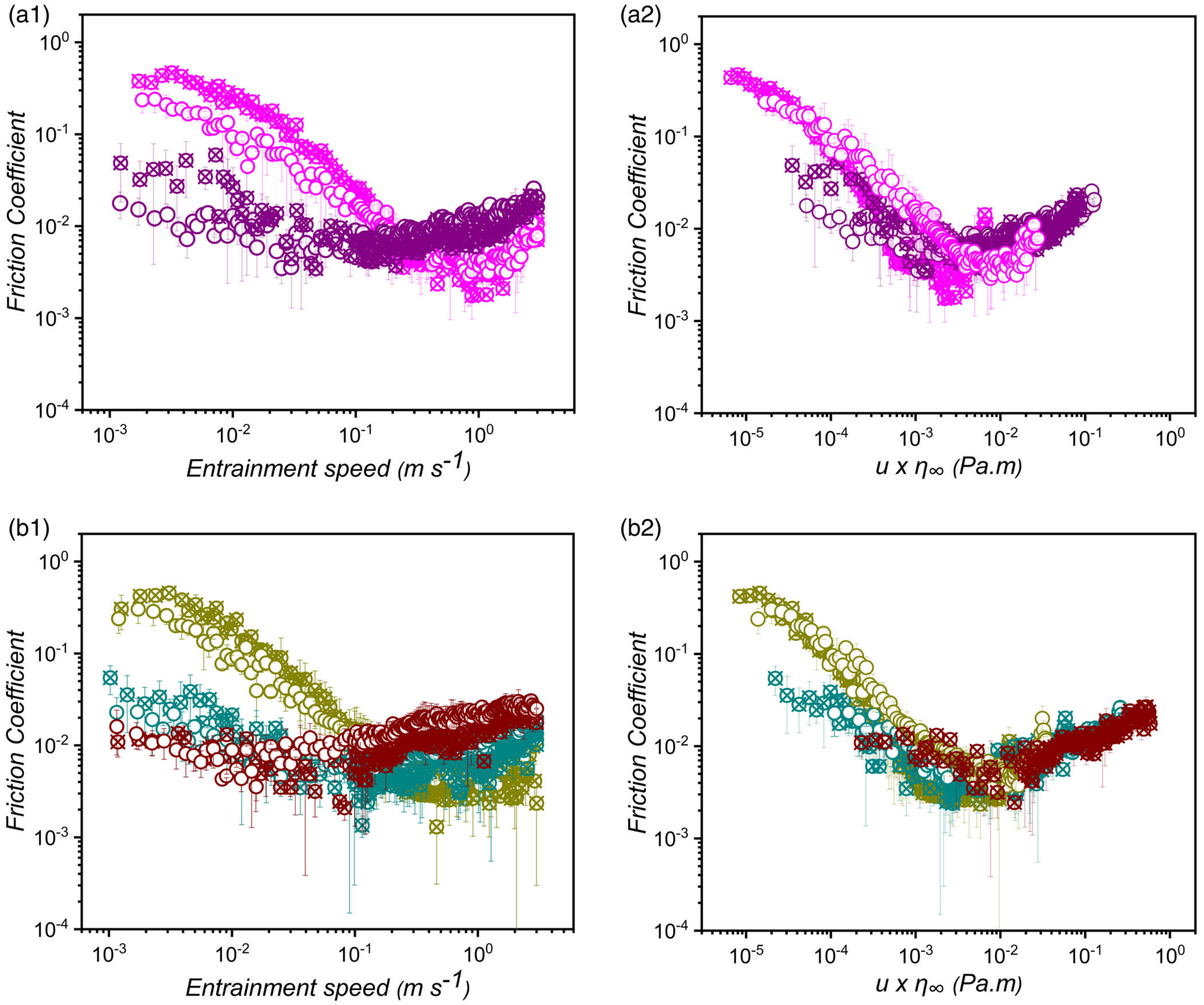

FIGURE 6 Friction coefficient (μ) results for biopolymer mixtures of potato protein and pectin, and their conjugated solutions at a potato protein to pectin ratio of (a$_1$ and a$_2$) 1:1 w/w (Po[0.5] + Pe[0.5] ○, Conj$_{1:1}$(Po[0.5] + Pe[0.5]) ⊠, Po[2.5] + Pe[2.5] ○, Conj$_{1:1}$(Po[2.5] + Pe[2. 5]) ⊠), and (b$_1$ and b$_2$) 1:2 w/w (Po[0.5] + Pe[1] ○, Conj$_{1:2}$(Po[0.5] + Pe[1]) ⊠, Po[1.25] + Pe[2.5] ○, Conj$_{1:2}$(Po[1.25] + Pe[2. 5]) ⊠, Po[2.5] + Pe[5] ○, Conj$_{1:2}$(Po[2.5] + Pe[5]) ⊠). The μ results are presented as a function of (a$_1$ and b$_1$) entrainment speed, u or (a$_2$ and b$_2$) the product of entrainment speed and high-shear rate viscosity, $u \times \eta_\infty$. Data represent means and standard deviations for three measurements for at least two independent samples ($n = 3 \times 2$).

upon addition to Po solutions. At both ratios, an increase in the concentration of Pe and/or Po appeared to shift the $\dot{\gamma}$ at which the η leveled off to higher values, to an extent that no apparent high-shear rate plateau was observed for the solutions with the highest concentration of Pe (i.e., 5 wt%). This can be attributed to a greater extent of intermolecular interactions at the higher concentration of Pe and Po which required a higher magnitude of $\dot{\gamma}$ to rupture. Further, most conjugated solutions exhibited an earlier onset of the plateau as compared to the corresponding unconjugated mixtures (Figure 5a,b). We hypothesized that the earlier onset of the plateau might be attributed to the condensation reaction in the conjugated solutions making it difficult to reorganize even at high shear rates (Tamnak et al., 2016). In addition, increased negative charges (shown in Table 2) after conjugation leads to strong repulsive protein–protein interactions, which are easier to be ruptured at weaker shear forces, with samples easier to flow.

The influence of Po:Pe ratio on the lubrication behavior of Po-Pe conjugates

The $\mu - u$ graphs at Po:Pe ratios of 1:1 and 1:2 w/w are plotted in Figure 6a$_1$,b$_1$, all showing that conjugation slightly increased μ at the boundary and mixed regimes under the conditions defined in this study ($p < 0.05$, except for Po[2.5] + Pe[5] vs. Conj$_{1:2}$(Po[2.5] + Pe[5])). As mentioned before, this observation can be attributed to the enhanced viscous lubricity provided by higher η values of the mixtures (Figure 5). The relative increase in μ appeared to be less pronounced at the lower ratio of Po:Pe (1:2) but did not show a conclusive dependency on the concentration of the biopolymers.

To further elucidate the contribution of viscous factor, we plotted the $\mu - u \times \eta_\infty$ graphs (η at $\dot{\gamma} = 1000\ \text{s}^{-1}$ was considered as η_∞) for Po:Pe ratios of 1:1 and 1:2 in Figure 6a_2,b_2, respectively. As can be seen at a given Po:Pe ratio, μ values across the EHL and HDL regimes were collapsed into a single curve showing negligible or no influence of conjugation and the biopolymer concentrations on the μ values at the EHL and HDL regimes. At the mixed regime, an increased biopolymer concentration led to lower μ values, suggesting slower kinetics of squeeze-out and de-wetting of the biopolymer films at the contact interface (Selway et al., 2017). With regard to the influence of conjugation, an opposite trend to that of $\mu - u$ graphs (Figure 6a_1,b_1) was observed at the mixed and boundary regimes. At Po:Pe ratio of 1:1 w/w and [Pe or Po]: 0.5 wt%, conjugates showed slightly lower ($p < 0.05$) or comparable μ values (depending on u) at the mixed regime. At Po:Pe ratio of 1:1 w/w and [Pe or Po]: 2.5 wt %, conjugation showed a trivial or slightly enhancing effect ($p < 0.05$) on μ depending on u. Conjugated mixtures at Po:Pe ratio of 1:2 w/w showed consistently comparable ($p > 0.05$) μ values to those of the corresponding mixtures. This evidences the obvious benefits of conjugation of Po with Pe at high DC% on lubrication properties and structural stability of the Po + Pe mixtures and Po solutions. The consistency with the lower Po:Pe ratio (i.e., higher DC%) implies a more effective interaction between PDMS and conjugated biopolymers or adsorption at the contact interface. The exact reasoning for this observation is not clear, however, it can be attributed to the heat-induced structural change of proteins (e.g., unfolding) which has been reported to expose hydrophobic groups (Ma, Hou, et al., 2020) and facilitate enhanced surface adsorption onto the PDMS surfaces.

CONCLUSIONS

A transition toward plant protein-rich foods appears to be a vital step to meet the sustainability targets in food formulation due to the environmental and ethical concerns over animal-sourced foods. Often plant protein-rich foods suffer from undesirable sensory perceptions such as dry, gritty, and rough mouthfeel, originating from poor lubrication performance, limiting their consumer acceptability. We hypothesize that a viable approach is to combine plant proteins with polysaccharides to generate plant protein-rich foods with enhanced lubrication-dependent attributes such as smooth and juicy mouthfeel. This study explored the flow and lubrication behavior of plant protein and polysaccharide by mixing or conjugation in an attempt toward the transition to sustainable, pleasurable plant-based food product design. Pectin (Pe) and potato protein (Po) as the model plant-based polysaccharides and proteins were selected. A clear benefit of Pe was appreciated in Po-Pe mixture and conjugates in both viscosity enhancement and friction reduction versus sole components. Conjugation resulted in formation of stable negatively-charged components. Particularly, when a reduced entrainment speed parameter was used to normalize the influence of viscosity, negatively-charged stable conjugates showed enhanced boundary and mixed lubrication performance as compared to Po, however, distinct advantage over unconjugated mixtures on lubrication performance was not obvious. In summary, this study suggests that Maillard-type conjugation, with no extraneous chemicals, can impart some degree of beneficial lubrication properties to Po by bringing Pe to offer viscous and boundary-film lubrication in a stable negatively-charged Po-Pe conjugated structure which shows promise to improve textural attributes of food products. The findings from this feasibility study suggest future prospects of using conjugation as a process to create new ingredient building blocks to produce sustainable plant-based food products with desirable textural attributes, which needs validation by sensory evaluation.

AUTHOR CONTRIBUTIONS

Anwesha Sarkar and Siavash Soltanahmadi conceived and designed the study. Mingxin Wang, Mohd Khalid Gul, and Siavash Soltanahmadi wrote the first draft of the manuscript. Mingxin Wang, Ecaterina Stribiţcaia, and Mohd Khalid Gul carried out the experiments, Siavash Soltanahmadi and Mingxin Wang analyzed the data. All authors contributed to and approved the final draft of the manuscript.

ACKNOWLEDGMENTS

This study was funded by Michael Beverley Innovation Fellowship, the European Research Council (ERC) under the European Union's Horizon 2020 Research and Innovation Programme (Grant agreement n° 757993) and UKRI under the UK guarantee for EU funding (Grant agreement n° EP/X03514X/1). Author MKG acknowledges funding from the Science and Engineering Research Board (SERB), Department of Science and Technology, Government of India, for his visiting research at the University of Leeds, UK through the SIRE fellowship.

CONFLICT OF INTEREST STATEMENT

The authors declare that they have no conflict of interest.

ETHICS STATEMENT

No human or animal subjects were used in this research.

ORCID

Anwesha Sarkar https://orcid.org/0000-0003-1742-2122

REFERENCES

Al-Hakkak J, Al-Hakkak F. Functional egg white–pectin conjugates prepared by controlled Maillard reaction. J Food Eng. 2010;100:152–9. https://doi.org/10.1016/j.jfoodeng.2010.03.040

Alves AC, Tavares GM. Mixing animal and plant proteins: is this a way to improve protein techno-functionalities? Food Hydrocoll. 2019;97:105171. https://doi.org/10.1016/j.foodhyd.2019.06.016

Araiza-Calahorra A, Glover ZJ, Akhtar M, Sarkar A. Conjugate microgel-stabilized Pickering emulsions: role in delaying gastric digestion. Food Hydrocoll. 2020;105:105794. https://doi.org/10.1016/j.foodhyd.2020.105794

Araiza-Calahorra A, Mackie AR, Feron G, Sarkar A. Can tribology be a tool to help tailor food for elderly population? Curr Opin Food Sci. 2023;49:100968. https://doi.org/10.1016/j.cofs.2022.100968

Batchelor H, Venables R, Marriott J, Mills T. The application of tribology in assessing texture perception of oral liquid medicines. Int J Pharm. 2015;479:277–81. https://doi.org/10.1016/j.ijpharm.2015.01.004

Biegler M, Delius J, Käsdorf BT, Hofmann T, Lieleg O. Cationic astringents alter the tribological and rheological properties of human saliva and salivary mucin solutions. Biotribology. 2016;6:12–20. https://doi.org/10.1016/j.biotri.2016.03.002

Brown FN, Mackie AR, He Q, Branch A, Sarkar A. Protein–saliva interactions: a systematic review. Food Funct. 2021;12:3324–51. https://doi.org/10.1039/D0FO03180A

Castellanos MM, Pathak JA, Colby RH. Both protein adsorption and aggregation contribute to shear yielding and viscosity increase in protein solutions. Soft Matter. 2014;10:122–31. https://doi.org/10.1039/C3SM51994E

de Vicente J, Stokes JR, Spikes HA. The frictional properties of Newtonian fluids in rolling–sliding soft-EHL contact. Tribol Lett. 2005;20:273–86. https://doi.org/10.1007/s11249-005-9067-3

Douglas TEL, Hempel U, Żydek J, Vladescu A, Pietryga K, Kaeswurm JAH, et al. Pectin coatings on titanium alloy scaffolds produced by additive manufacturing: promotion of human bone marrow stromal cell proliferation. Mater Lett. 2018;227:225–8. https://doi.org/10.1016/j.matlet.2018.05.060

Einhorn-Stoll U, Ulbrich M, Sever S, Kunzek H. Formation of milk protein–pectin conjugates with improved emulsifying properties by controlled dry heating. Food Hydrocoll. 2005;19:329–40. https://doi.org/10.1016/j.foodhyd.2004.07.005

Fan Y, Yi J, Zhang Y, Yokoyama W. Fabrication of curcumin-loaded bovine serum albumin (BSA)-dextran nanoparticles and the cellular antioxidant activity. Food Chem. 2018;239:1210–8. https://doi.org/10.1016/j.foodchem.2017.07.075

Fu Y, Liu W-N, Soladoye OP. Towards potato protein utilisation: insights into separation, functionality and bioactivity of patatin. Int J Food Sci Technol. 2020;55:2314–22. https://doi.org/10.1111/ijfs.14343

Gentile L. Protein–polysaccharide interactions and aggregates in food formulations. Curr Opin Colloid Interface Sci. 2020;48:18–27. https://doi.org/10.1016/j.cocis.2020.03.002

Goh KKT, Teo A, Sarkar A, Singh H. Chapter 13 – Milk protein-polysaccharide interactions. In: Boland M, Singh H, editors. Milk proteins. 3rd ed. Academic Press: London, UK; 2020. p. 499–535.

Hu J, Andablo-Reyes E, Soltanahmadi S, Sarkar A. Synergistic microgel-reinforced hydrogels as high-performance lubricants. ACS Macro Lett. 2020;9:1726–31. https://doi.org/10.1021/acsmacrolett.0c00689

Hussain M, Qayum A, Xiuxiu Z, Liu L, Hussain K, Yue P, et al. Potato protein: an emerging source of high quality and allergy free protein, and its possible future based products. Food Res Int. 2021;148:110583. https://doi.org/10.1016/j.foodres.2021.110583

Inglett GE, Chen D, Liu SX. Functional properties of teff and oat composites. Food Nutr Sci. 2015;6:1591–602. https://doi.org/10.4236/fns.2015.617164

Itkonen ST, Päivärinta E, Pellinen T, Viitakangas H, Risteli J, Erkkola M, et al. Partial replacement of animal proteins with plant proteins for 12 weeks accelerates bone turnover among healthy adults: a randomized clinical trial. J Nutr. 2021;151:11–9. https://doi.org/10.1093/jn/nxaa264

Kew B, Holmes M, Stieger M, Sarkar A. Oral tribology, adsorption and rheology of alternative food proteins. Food Hydrocoll. 2021;116:106636. https://doi.org/10.1016/j.foodhyd.2021.106636

Laguna L, Sarkar A. Oral tribology: update on the relevance to study astringency in wines. Tribol Mater Surf Interfaces. 2017;11:116–23. https://doi.org/10.1080/17515831.2017.1347736

Lan Y, Ohm J-B, Chen B, Rao J. Phase behavior, thermodynamic and microstructure of concentrated pea protein isolate-pectin mixture: effect of pH, biopolymer ratio and pectin charge density. Food Hydrocoll. 2020;101:105556. https://doi.org/10.1016/j.foodhyd.2019.105556

Li M, Blecker C, Karboune S. Molecular and air-water interfacial properties of potato protein upon modification via laccase-catalyzed cross-linking and conjugation with sugar beet pectin. Food Hydrocoll. 2021;112:106236. https://doi.org/10.1016/j.foodhyd.2020.106236

Li X, Al-Assaf S, Fang Y, Phillips GO. Characterisation of commercial LM-pectin in aqueous solution. Carbohydr Polym. 2013;92:1133–42. https://doi.org/10.1016/j.carbpol.2012.09.100

Lutz R, Aserin A, Portnoy Y, Gottlieb M, Garti N. On the confocal images and the rheology of whey protein isolated and modified pectins associated complex. Colloids Surf B Biointerfaces. 2009;69:43–50. https://doi.org/10.1016/j.colsurfb.2008.10.011

Ma X, Chen W, Yan T, Wang D, Hou F, Miao S, et al. Comparison of citrus pectin and apple pectin in conjugation with soy protein isolate (SPI) under controlled dry-heating conditions. Food Chem. 2020;309:125501. https://doi.org/10.1016/j.foodchem.2019.125501

Ma X, Chi C, Pu Y, Miao S, Liu D. Conjugation of soy protein isolate (SPI) with pectin: effects of structural modification of the grafting polysaccharide. Food Chem. 2022;387:132876. https://doi.org/10.1016/j.foodchem.2022.132876

Ma X, Hou F, Zhao H, Wang D, Chen W, Miao S, et al. Conjugation of soy protein isolate (SPI) with pectin by ultrasound treatment. Food Hydrocoll. 2020;108:106056. https://doi.org/10.1016/j.foodhyd.2020.106056

Mao Y, Huang M, Bi J, Sun D, Li H, Yang H. Effects of kappa-carrageenan on egg white ovalbumin for enhancing the gelation and rheological properties via electrostatic interactions. Food Hydrocoll. 2023;134:108031. https://doi.org/10.1016/j.foodhyd.2022.108031

Martins SIFS, Jongen WMF, van Boekel MAJS. A review of Maillard reaction in food and implications to kinetic modelling. Trends Food Sci Technol. 2000;11:364–73. https://doi.org/10.1016/S0924-2244(01)00022-X

Morris ER, Richardson RK, Taylor LJ. Correlation of the perceived texture of random coil polysaccharide solutions with objective parameters. Carbohydr Polym. 1984;4:175–91. https://doi.org/10.1016/0144-8617(84)90010-9

Naik RR, Wang Y, Selomulya C. Improvements of plant protein functionalities by Maillard conjugation and Maillard reaction products. Crit Rev Food Sci Nutr. 2022;62:7036–61. https://doi.org/10.1080/10408398.2021.1910139

Nielsen PM, Petersen D, Dambmann C. Improved method for determining food protein degree of hydrolysis. J Food Sci. 2001;66:642–6. https://doi.org/10.1111/j.1365-2621.2001.tb04614.x

Pang Z, Tong F, Jiang S, Chen C, Liu X. Particle characteristics and tribo-rheological properties of soy protein isolate (SPI) dispersions: effect of heating and incorporation of flaxseed gum. Int J Biol Macromol. 2023;232:123455. https://doi.org/10.1016/j.ijbiomac.2023.123455

Pradal C, Stokes JR. Oral tribology: bridging the gap between physical measurements and sensory experience. Curr Opin Food Sci. 2016;9:34–41. https://doi.org/10.1016/j.cofs.2016.04.008

Qi PX, Xiao Y, Wickham ED. Changes in physical, chemical and functional properties of whey protein isolate (WPI) and sugar beet pectin (SBP) conjugates formed by controlled dry-heating. Food Hydrocoll. 2017;69:86–96. https://doi.org/10.1016/j.foodhyd.2017.01.032

Saint-Eve A, Granda P, Legay G, Cuvelier G, Delarue J. Consumer acceptance and sensory drivers of liking for high plant protein snacks. J Sci Food Agric. 2019;99:3983–91. https://doi.org/10.1002/jsfa.9624

Sarkar A, Andablo-Reyes E, Bryant M, Dowson D, Neville A. Lubrication of soft oral surfaces. Curr Opin Colloid Interface Sci. 2019;39:61–75. https://doi.org/10.1016/j.cocis.2019.01.008

Sarkar A, Soltanahmadi S, Chen J, Stokes JR. Oral tribology: providing insight into oral processing of food colloids. Food Hydrocoll. 2021;117:106635. https://doi.org/10.1016/j.foodhyd.2021.106635

Schmidt JM, Damgaard H, Greve-Poulsen M, Sunds AV, Larsen LB, Hammershøj M. Gel properties of potato protein and the isolated fractions of patatins and protease inhibitors – impact of drying method, protein concentration, pH and ionic strength. Food Hydrocoll. 2019;96:246–58. https://doi.org/10.1016/j.foodhyd.2019.05.022

Seggiani M, Puccini M, Pierini M, Giovando S, Forneris C. Effect of different extraction and precipitation methods on yield and quality of pectin. Int J Food Sci Technol. 2009;44:574–80. https://doi.org/10.1111/j.1365-2621.2008.01849.x

Selway N, Chan V, Stokes JR. Influence of fluid viscosity and wetting on multiscale viscoelastic lubrication in soft tribological contacts. Soft Matter. 2017;13:1702–15. https://doi.org/10.1039/C6SM02417C

Setiowati AD, Vermeir L, Martins J, De Meulenaer B, Van der Meeren P. Improved heat stability of protein solutions and O/W emulsions upon dry heat treatment of whey protein isolate in the presence of low-methoxyl pectin. Colloids Surf A Physicochem Eng Asp. 2016;510:93–103. https://doi.org/10.1016/j.colsurfa.2016.05.034

Shewan HM, Pradal C, Stokes JR. Tribology and its growing use toward the study of food oral processing and sensory perception. J Texture Stud. 2020;51:7–22. https://doi.org/10.1111/jtxs.12452

Soltanahmadi S, Bryant M, Sarkar A. Insights into the multiscale lubrication mechanism of edible phase change materials. ACS Appl Mater Interfaces. 2023;15:3699–712. https://doi.org/10.1021/acsami.2c13017

Soltanahmadi S, Murray BS, Sarkar A. Comparison of oral tribological performance of proteinaceous microgel systems with protein-polysaccharide combinations. Food Hydrocoll. 2022;129:107660. https://doi.org/10.1016/j.foodhyd.2022.107660

Souza CJF, Garcia-Rojas EE. Interpolymeric complexing between egg white proteins and xanthan gum: effect of salt and protein/polysaccharide ratio. Food Hydrocoll. 2017;66:268–75. https://doi.org/10.1016/j.foodhyd.2016.11.032

Sriamornsak P, Wattanakorn N, Takeuchi H. Study on the mucoadhesion mechanism of pectin by atomic force microscopy and mucin-particle method. Carbohydr Polym. 2010;79:54–9. https://doi.org/10.1016/j.carbpol.2009.07.018

Stokes JR, Boehm MW, Baier SK. Oral processing, texture and mouthfeel: from rheology to tribology and beyond. Curr Opin Colloid Interface Sci. 2013;18:349–59. https://doi.org/10.1016/j.cocis.2013.04.010

Stokes JR, Macakova L, Chojnicka-Paszun A, de Kruif CG, de Jongh HHJ. Lubrication, adsorption, and rheology of aqueous polysaccharide solutions. Langmuir. 2011;27:3474–84. https://doi.org/10.1021/la104040d

Tamnak S, Mirhosseini H, Tan CP, Ghazali HM, Muhammad K. Physicochemical properties, rheological behavior and morphology of pectin-pea protein isolate mixtures and conjugates in aqueous system and oil in water emulsion. Food Hydrocoll. 2016;56:405–16. https://doi.org/10.1016/j.foodhyd.2015.12.033

Tiwari BK, Muthukumarappan K, O'Donnell CP, Cullen PJ. Rheological properties of sonicated guar, xanthan and pectin dispersions. Int J Food Prop. 2010;13:223–33. https://doi.org/10.1080/10942910802317610

Torres O, Yamada A, Rigby NM, Hanawa T, Kawano Y, Sarkar A. Gellan gum: a new member in the dysphagia thickener family. Biotribology. 2019;17:8–18. https://doi.org/10.1016/j.biotri.2019.02.002

Vlădescu S-C, Agurto MG, Myant C, Boehm MW, Baier SK, Yakubov GE, et al. Protein-induced delubrication: how plant-based and dairy proteins affect mouthfeel. Food Hydrocoll. 2023;134:107975. https://doi.org/10.1016/j.foodhyd.2022.107975

Wang P, Sun G, Lu P, Liu Y, Zhu Y, Chen F. Mitigation effects of high methoxyl pectin on acrylamide formation in the Maillard model system. Food Chem. 2022;378:132095. https://doi.org/10.1016/j.foodchem.2022.132095

Wefers D, Bindereif B, Karbstein HP, van der Schaaf US. Whey protein-pectin conjugates: linking the improved emulsifying properties to molecular and physico-chemical characteristics. Food Hydrocoll. 2018;85:257–66. https://doi.org/10.1016/j.foodhyd.2018.06.030

Wijaya W, Patel AR, Setiowati AD, Van der Meeren P. Functional colloids from proteins and polysaccharides for food applications. Trends Food Sci Technol. 2017;68:56–69. https://doi.org/10.1016/j.tifs.2017.08.003

Xu F, Liamas E, Bryant M, Adedeji AF, Andablo-Reyes E, Castronovo M, et al. A self-assembled binary protein model explains high-performance salivary lubrication from macro to nanoscale. Adv Mater Interfaces. 2020;7:1901549. https://doi.org/10.1002/admi.201901549

Yadav MP, Strahan GD, Mukhopadhyay S, Hotchkiss AT, Hicks KB. Formation of corn fiber gum–milk protein conjugates and their molecular characterization. Food Hydrocoll. 2012;26:326–33. https://doi.org/10.1016/j.foodhyd.2011.02.032

Yao X, McClements DJ, Su Y, Li J, Chang C, Wang J, et al. Fabrication, structural and emulsifying properties of egg white protein-dextran conjugates through Maillard reaction. Food Biophys. 2022;17:650–61. https://doi.org/10.1007/s11483-022-09745-8

You K-M, Murray BS, Sarkar A. Rheology and tribology of starch + κ-carrageenan mixtures. J Texture Stud. 2021;52:16–24. https://doi.org/10.1111/jtxs.12570

You K-M, Murray BS, Sarkar A. Tribology and rheology of water-in-water emulsions stabilized by whey protein microgels. Food Hydrocoll. 2023;134:108009. https://doi.org/10.1016/j.foodhyd.2022.108009

You K-M, Sarkar A. Chapter 4 – Oral tribology of polysaccharides. In: Phillips GO, Williams PA, editors. Handbook of hydrocolloids. 3rd ed. Woodhead Publishing: London, UK; 2021. p. 93–124.

Zembyla M, Liamas E, Andablo-Reyes E, Gu K, Krop EM, Kew B, et al. Surface adsorption and lubrication properties of plant and dairy proteins: a comparative study. Food Hydrocoll. 2021;111:106364. https://doi.org/10.1016/j.foodhyd.2020.106364

Zundel J, Ansari SA, Trivedi HM, Masters JG, Mascaro S. Characterization of friction and moisture of porcine lingual tissue in vitro in response to artificial saliva and mouthwash solutions. Skin Res Technol. 2018;24:642–9. https://doi.org/10.1111/srt.12579

How to cite this article: Soltanahmadi S, Wang M, Gul MK, Stribiţcaia E, Sarkar A. Tribology and rheology of potato protein and pectin mixtures and Maillard conjugates. Sust Food Prot. 2023;1(4):149–63. https://doi.org/10.1002/sfp2.1018